Analysis of traditional windcatchers and the effects produced by changing the size, shape, and position of the outlet opening

C.A. Varela-Boydo [a,*], S.L. Moya [a], R. Watkins [b]

[a] Tecnologico Nacional de México, Centro Nacional de Investigacion y Desarrollo Tecnol´ ogico, Interior Internado Palmira S/n, Colonia Palmira, Cuernavaca, 62490, ´ Morelos, Mexico [b] Kent School of Architecture & Planning, University of Kent, United Kingdom

Increased thermal comfort in buildings is consuming large amounts of energy around the world, especially in hot arid and semi-arid regions. Finding and adapting ways to naturally cool buildings should be a priority for researchers in the subject. For centuries the Middle East cultures have used wind towers to cool their buildings and they have proved to be a cost-effective, easy to implement and reliable solution for passive cooling that requires almost negligible energy to operate. The present work tests one traditional windcatcher and 33 modifications of the design of the outlet opening. It seeks to act as a guide to how both to enhance and also avoid reducing performance when designing windcatchers with traditional designs. Using CFD modelling, the volumetric airflow that was captured by the catcher was computed for the different outlet modifications, and this revealed which designs restrain the flow and which boost the airflow, making the wind towers more effective.

1. Introduction

The use of energy in buildings accounts for some 40% of global energy consumption and greenhouse gas emissions. In addition, 30% of global electricity is used in buildings and this is projected to grow to 70% by 2050 [1]. More than 60% of all the energy consumed in building sector is used in heating, ventilation and air conditioning systems [1]. Depending on the country and the season, the amount and type of energy consumed can change. For instance, in hot regions, the electricity used by air conditioning systems is higher, mainly during the summer, with the consequent economic and environmental impacts that accompany this. For the residential sector in hot climates, the energy consumption dedicated for cooling purposes can range from 2% to 7% [2], and is expected to increase to 35% in 2050 and even 61% in 2100 [2], caused by global warming effects, the increase of the economic activities and the global population growth. This consumption could decrease significantly if buildings were designed taking into consideration their geographical location, the climate conditions, wind speeds, predominant wind directions, the most suitable materials in terms of their thermal properties, and by incorporating passive systems for natural ventilation [3,4], among other factors.

The traditional architecture of some Middle Eastern cultures offers examples of very ingenious solutions for the thermal comfort problems that the climates of those regions present to the interior of the buildings; such is the case of the passive system for natural ventilation called Wind Tower or Windcatcher, but also known as Badgir, Badhanj, Malqaf, among many other names depending of the country or region were they are used and their design. In general, these systems are vertical structures with one or several channels in their interior and integrated into the buildings. In their upper part, there are apertures oriented in the direction of prevailing winds to facilitate their capture. Once the wind has been captured, it flows through smaller cross-section channels, increasing the speed of the captured air, which is then channeled through the building, providing comfort to the occupants without the need for the use of electromechanical air conditioners. According to bibliography, wind towers have been in use for at least 3000 years. Its use can be traced to ancient Egyptians, mainly in Cairo, and the early Assyrian culture, in modern Iraq [5]. In Iraq, they can be found over a large portion of the territory and they are considered as an architecture masterpiece of the ancient times. However, the city of Yazd stands out for the considerable amount of windcatchers of different types and shapes that are spread over the city. Their designs can be as diverse as the number of openings present in the towers. The can range from a single opening to hexahedral designs with multiple openings [6].

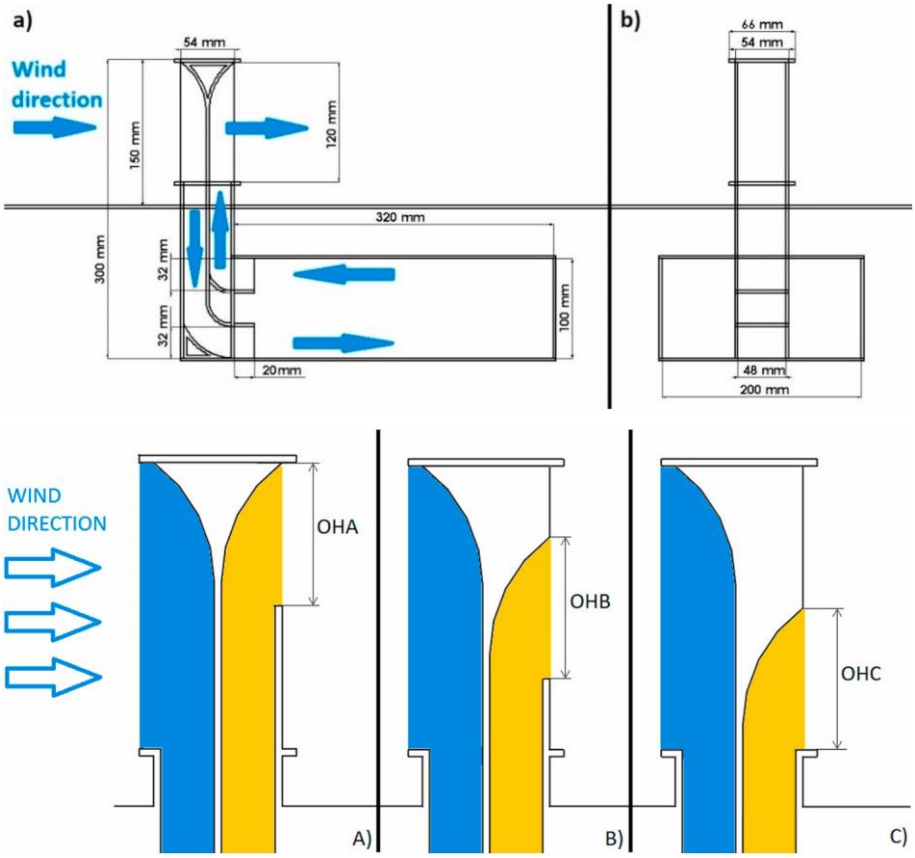

Fig. 2. Designs for outlet configurations A, B, C.

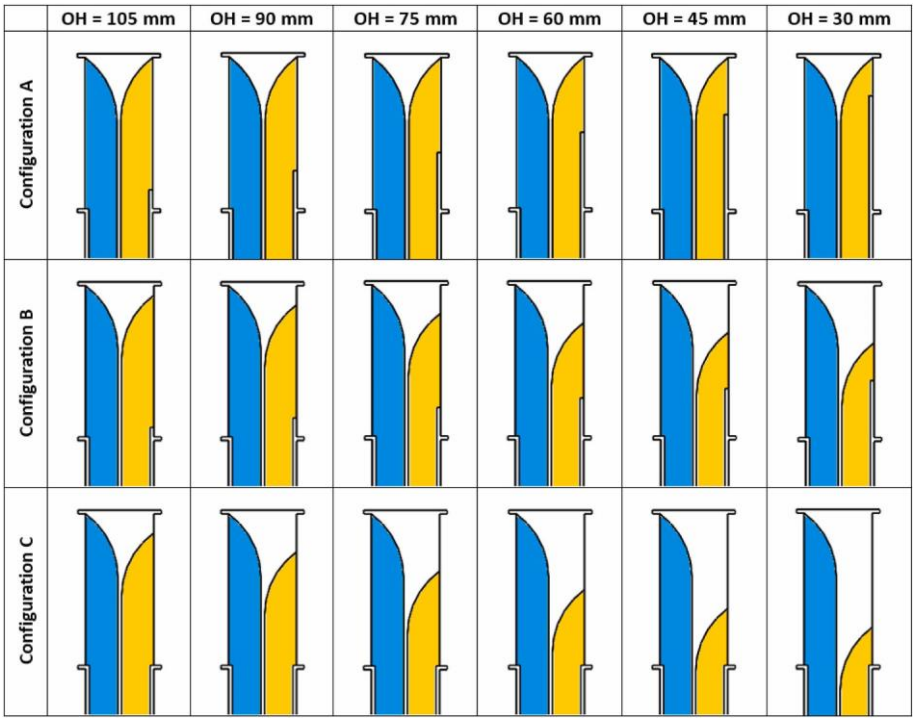

Fig. 3. All the geometric configurations used for A, B, C.

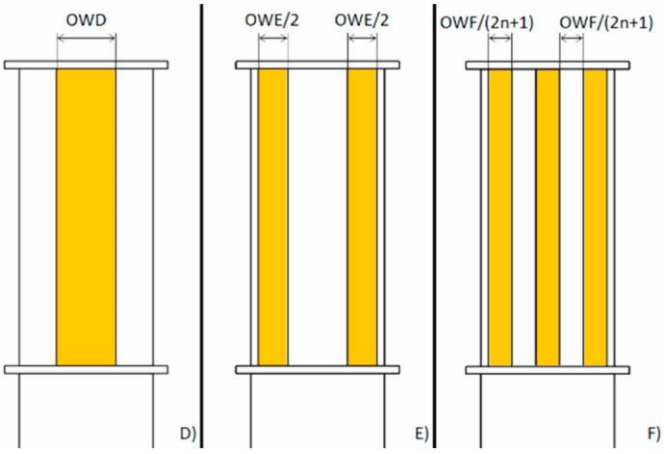

Fig. 4. Designs for outlet configurations D, E, F.

A considerable body of work has been published on the operation and capacity of the different types of windcatchers to increase natural ventilation in buildings. Research that studies the functioning of the traditional windcatchers covers: (a) monitoring in buildings with windcatchers [7–9], (b) experiments with scale models in wind tunnels [10–14], supplemented with CFD, and (c) studies with CFD [15–22] at full size, generally made using commercial codes. The functioning of windcatchers is so convenient that many modern architectural designs seek their utilization. However, the present work focuses on the understanding and also the possibilities of improving the vernacular designs in a respectful way that can continue the style of traditional wind towers but with better performance. In this context, a great number of research papers have been published on the matter and a comprehensive classification of the traditional windcatchers based on their morphology is presented in Ref. [18]. In the same manuscript, the authors use CFD to compare the effects of different types of windcatchers on the indoor ventilation rate. A study that seeks to understand the basics of vernacular wind towers and their performance is [14]. This interesting research used wind tunnel testing and numerical simulations of a real four-sided wind tower with parlor and courtyard and published how different incident angles and speed of the wind affect the volumetric flow captured by the tower and its effects on the parlor. Considering basic tower designs, various manuscripts study the use of two opening windcatchers. One that works with traditional designs [23], studies around 300 configurations of internal modifications on the wind tower. By adding convergent-divergent nozzles, finned-curved inlet openings and by increasing the size of the dividers between inlet and outlet openings, they manage to increase induced mass flow. Also studying two sided catchers [24], found that the behavior of the flow outside of the buildings has an effect over the air distribution inside the building. They managed to quantify the differences in the air flow inside a building with a two sided windcatcher, having a smooth upstream fetch in comparison with a rough fetch. Aiming to improve the performance of the two openings windcatchers, some works have modify the exterior of the towers to boost performance. Windcatchers integrated with wing walls were studied to assess the changes in indoor air quality in a scale building. By simulating ten different lengths of wing walls, they found which configuration performs the best [25]. Also trying to improve performance in windcatchers, some of the authors of the present work published the use of inlet extension for the wind towers [26].

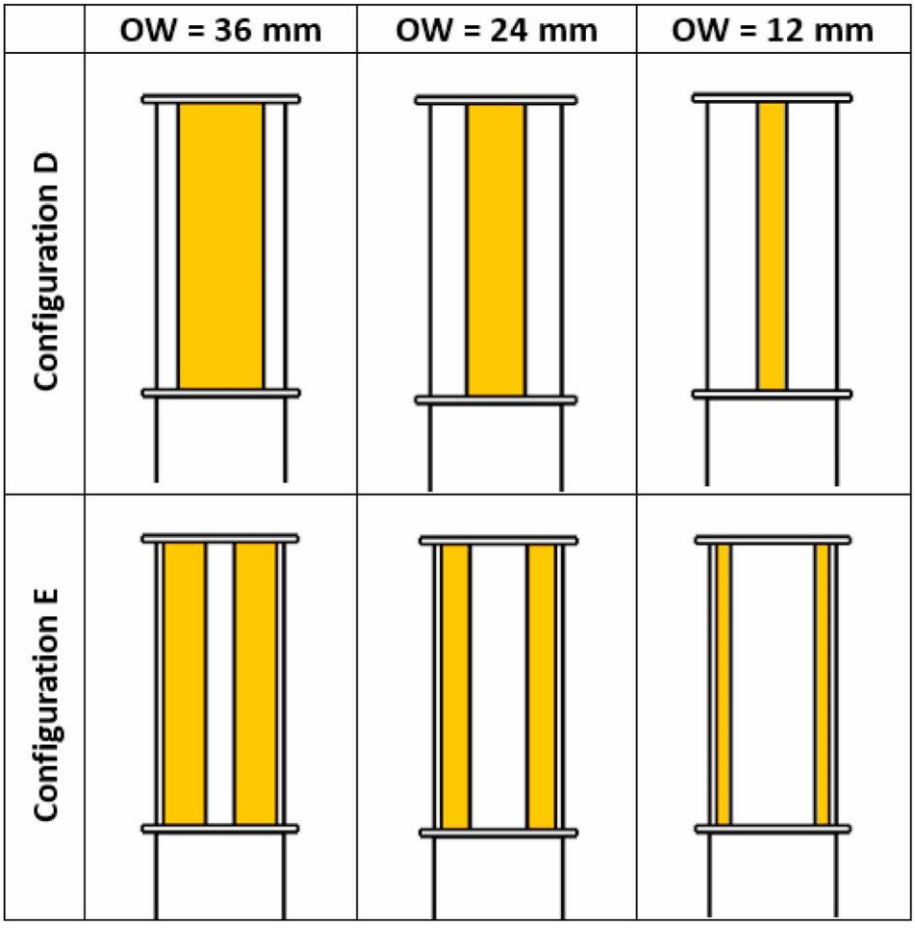

Fig. 5. Geometric configurations used for D, E.

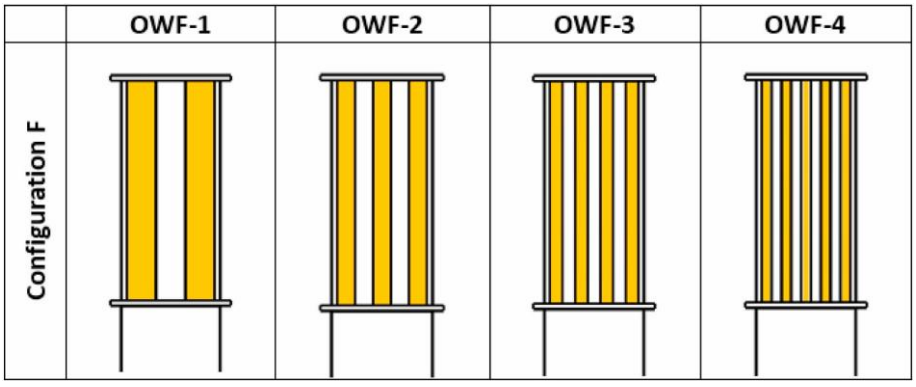

Fig. 6. Geometric configurations used for F.

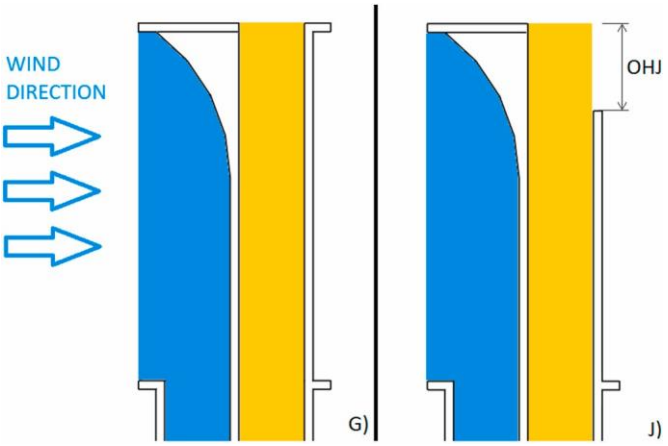

Fig. 7. Designs for outlet configurations G, J.

During wind tunnel testing and preliminary CFD simulations, it was found that almost half of the air inside the inlet openings of the wind towers formed an ascending current. This current takes air from inside the tower and creates a stream that evacuates air from the inlets. Different types of inlet extension were proposed to prevent the formation of these streams to improve performance.

For the present work the authors propose the study of windcatchers with two openings. As in Ref. [13], the use of one opening for air ingress and another for the air egress to and from the building is considered. In a similar fashion [10] conducts a remarkably similar study of catchers of the same kind in similar conditions. After wind tunnel testing and CFD simulations, both [10,13] studies, published that the wind direction has an extremely large influence on the windcatcher performance. At the same time, they conclude that the induced airflow rate increases as the wind speed in the atmosphere increases. In general, there are many studies that find the same conclusions, so for the present work, the use of one single wind direction is proposed, focusing the study on the towers' outlet opening modifications, aiming to find ways to reduce losses in the wind tower functioning. Various studies have sought improvements in the aerodynamic performance of windcatchers [27]. Showed the effect that changing the tower's height has over the air catching, finding that in the climate of Jordan the height necessary for the towers to work optimally is lower than the height used traditionally in the vernacular designs [20]. tested different geometric configurations of the inlets and showed that making improvements to the catcher can improve airflow inside the buildings. In a similar spirit [19], studied the effect that using different internal designs has over the overall performance when windcatchers are used in combinations with evaporative cooling techniques. Regarding the outlet opening that is the main focus of the present work [22], presents a very extensive research of different outlet configurations combining windows in the rooms, different locations for the catchers on the roofs of the buildings, among many other, documenting the resulting air quality over the several design iterations for buildings.

The present work is part of project that seeks to find ways to improve the functioning of wind catchers. In parallel studies different proposals are being tested. One of them studies the use of funnels attached to increase the opening area. Another [26], proposes the use of inlet extensions to boots induction. A fourth one studies catchers capable of redirecting to always face the wind. In the present study, a traditional windcatcher with a two opening configuration is proposed to test how the reduction in size, shape, and position of the outlet opening can reduce the performance of the air induction from the outside into the building. To evaluate the importance of the outlet design, 33 variations of the opening are presented and compared with the original design. Of

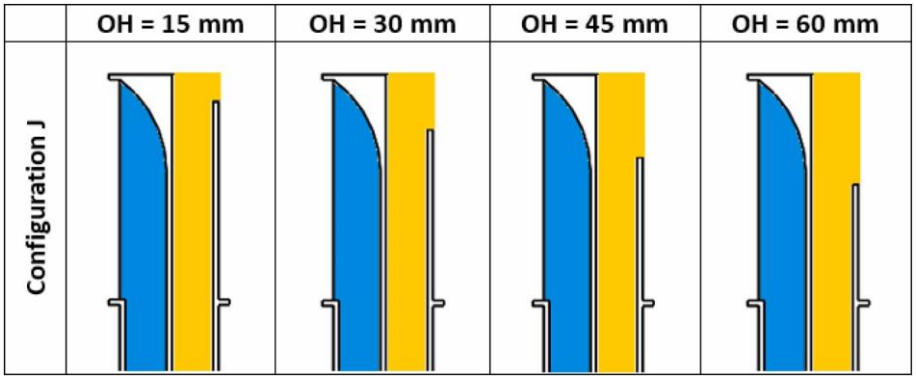

Fig. 8. Designs for outlet configuration J.

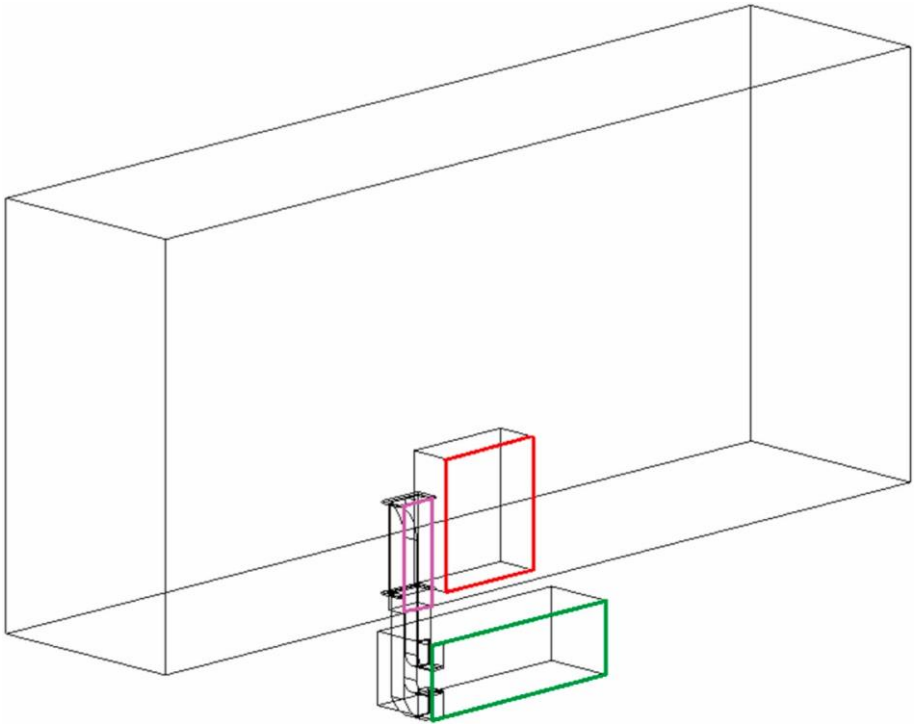

Fig. 9. Domain includes the windcatcher (in purple), the underground building (in green), and the wake control volume (in red). (For interpretation of the references to color in this figure legend, the reader is referred to the Web version of this article.)

Table 1
Element size for the mesh, see Fig. 10.

	Region	Size (meters)
(1)	Outer catcher wall	2.5e-5
(2)	Inner catcher ducts' wall	2.1e-5
(3)	Room/building wall	4.0e-3
(4)	Wake control wall	2.0e-3
(5)	Wake control volume	2.5e-3
(6)	Ground	5.0e-3

them, 18 test how reducing the area by using shorter heights and three different positions can reduce the flow. Moreover, six configurations where the width is reduced are presented. In the vernacular designs, the presence of columns in the apertures is documented. To test how the columns affect the performance, the model was augmented with different numbers of columns (1–4) and the difference in the flow going through the building computed. Finally, it is well known that when a fluid has to change direction quickly, a considerable amount of energy has to be used to overcome the inertia. To gauge the potential impact of reducing this, five different configurations where part of the tower's roof is removed are presented to evaluate the use of vertical outlets for the air exiting the building.

To analyze these phenomena, the results of 204 CFD cases are presented. They simulate at six free stream velocities the interactions of the air flowing in one single direction. This represents a different approach to studying windcatchers because in the majority of the previously mentioned manuscripts, just a few models are studied under different variables, while in the present work a great number of models are evaluated under fewer variations of the wind. The results from evaluating the original windcatcher and the 33 different modified towers with outlet variations can provide an understanding of how different sizes and shapes can affect windcatcher performance. This information can then be used to design new, more efficient catchers or to improve the existing ones.

2. Windcatcher geometry

The impact (in terms of volumetric airflow) of modifying the shape and size of the windcatcher outlet openings was determined for 34 different designs. All of these respected the basic traditional shape of the windcatchers. Commercial CAD software was used to create the geometries, and then these were exported to the ANSYS Workbench interface for further use. Various simplifications were made during the design phase. One of these was that the tower inlet would always be the air ingress and the outlet would only work as an exit for the air: in reality at this would mean that the catcher would be installed in an area with one predominant wind direction.

The most significant simplification consisted in testing only the top of the tower connected to an underground room or building, in order to test only the aerodynamics of the catcher, as can be seen in Fig. 1. Also, there were no walls or windows installed in the room, only one ingress duct and one egress duct, both with a 20 mm length inside the room. The dimensions in Fig. 1 represent a 1:25 scale model of a small

building tested in a wind tunnel. This configuration was selected following the results of parallel research done by the same authors. Were CFD simulations offered results with less that 5% of error between the calibrated numerical simulations and the wind tunnel tests.

Fig. 2 shows the middle plane of the tower parallel to the wind direction and shows the first three outlet configurations. Configurations A, B, C, are presented to test the impact that shortening the outlet height (OH) has over the volumetric flow. Ingress ducts are shown in blue and egress in orange. Configuration A changes the opening height (OHA) from the bottom to the top, and it decreases the opening from the original 120 mm–30 mm in decrements of 15 mm. Configuration B decreases the OH in the same decrements but it leaves the opening always in the middle, meaning that it closes the opening 7.5 mm from the bottom and 7.5 mm from the top every time. Configuration C works the same way but it closes the opening from the top to the bottom. Both configurations (B, C), drag the curved exit wall down as the outlet closes to avoid the formation of vortexes inside the outlet. Fig. 3 shows all the models from these 3 configurations.

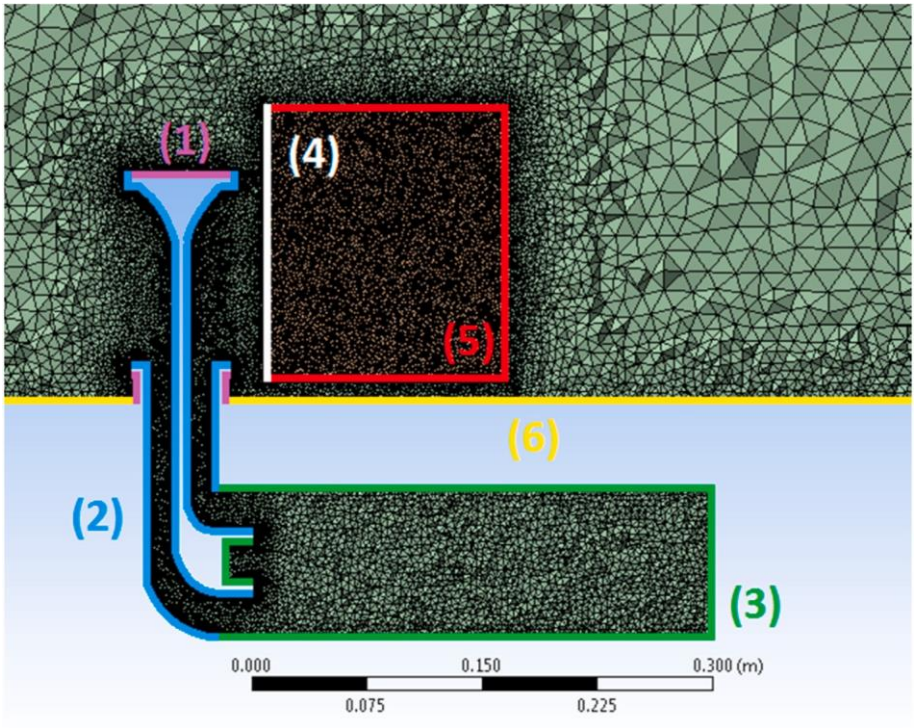

Fig. 10. Symmetry plane for the simulation showing a close view of the mesh elements and highlighting the different zones configured.

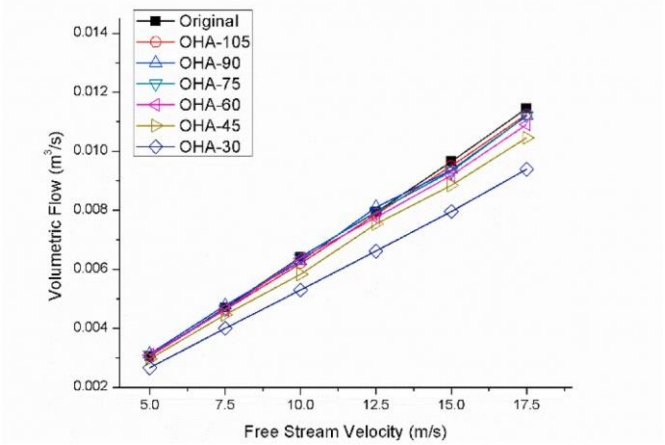

Fig. 11. Volumetric flow of the catchers with configuration A outlets at different free stream velocities.

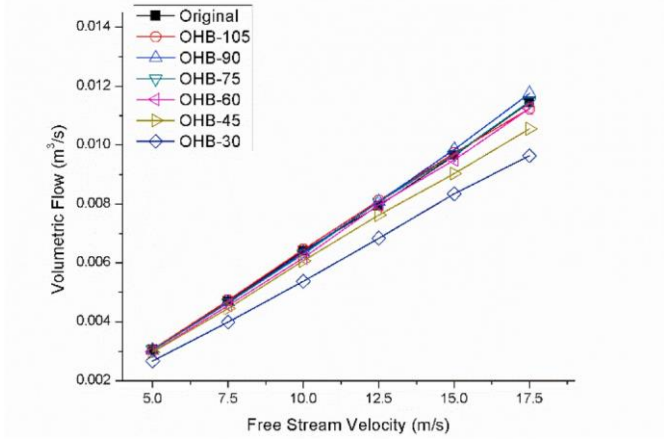

Fig. 12. Volumetric flow of the catchers with configuration B outlets at different free stream velocities.

Fig. 4 shows a view parallel to the domain's inlet looking towards the outlet openings of the windcatchers: three more configurations are shown with the outlets colored in orange. Configuration D is to study the effect of reducing the outlet width. It reduces the opening width (OWD) from the original 48 mm–12 mm in decrements of 12 mm from both sides to the center. Configuration E reduces the outlet in the same decrements but closes the opening from the center to the sides, having a solid element in the middle of the egress duct with the same thickness of the walls (3 mm). Configuration F seeks to replicate the columns installed in the vernacular designs of the traditional windcatchers. This configuration changes the number of columns (n) present in the tower from 1 to 4, with the width of the columns reducing as the number increases because they are equally spaced and have the same width as the hollow space between them. Figs. 5 and 6 show the 10 different models of configurations D, E, F, used during simulations.

These first six configurations (A-F) were tested to evaluate the reduction in the volumetric flow inside the ducts of the 28 tower model variations in order to avoid them in future research. In the search for different kinds of outlets, configurations G and J were considered and are shown in Fig. 7. They seek to take advantage of the low-pressure zone present at the top of the towers in order to boost the air evacuation from the building, and also to avoid the last change of direction of the air in order to have vertical outlets. This helps the flow by saving the energy needed to overcome the inertia of air when changing from a vertical to a horizontal direction inside the tower and instead delaying the change in direction until the air is outside of the building.

To accomplish this, configuration G has part of the roof of the tower removed and a complete closure of the original outlet, forcing the air to leave the duct vertically, perpendicular to the direction of the main wind direction (Fig. 7G). Configuration J (Fig. 7J) also removes part of the roof, but has the original outlet only partially closed. The outlet height for the J configuration (OHJ) was set from 15 mm to 60 mm in

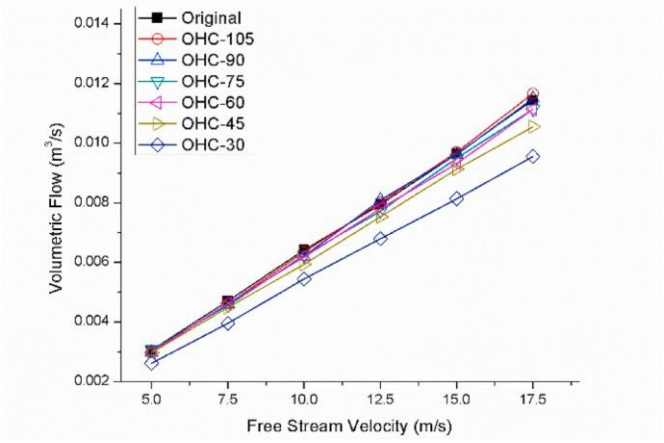

Fig. 13. Volumetric flow of the catchers with configuration C outlets at different free stream velocities.

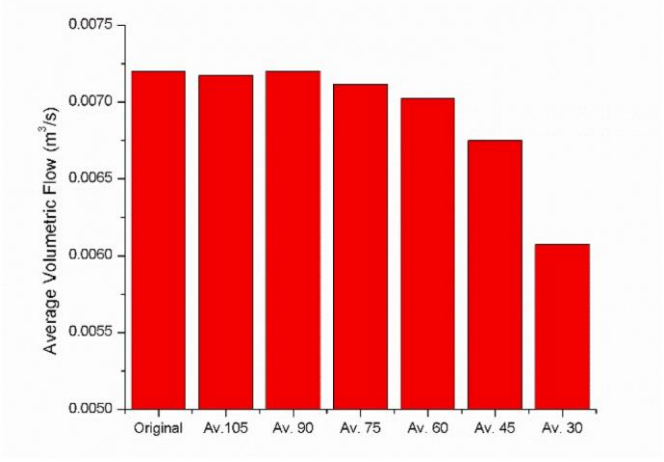

Fig. 14. Average volumetric flow for all the configurations at different length outlet openings.

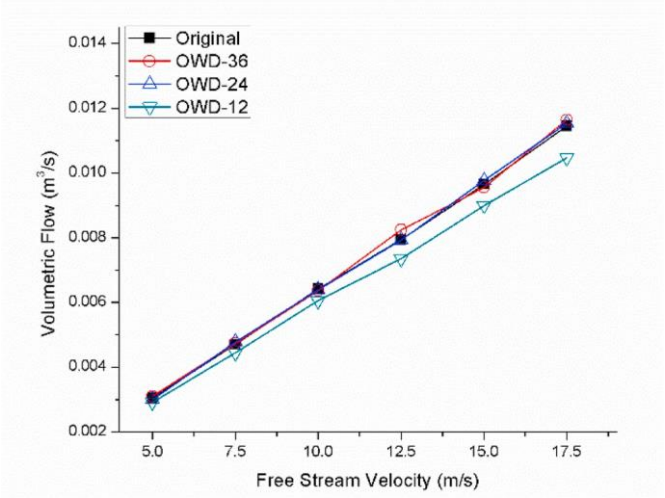

Fig. 15. Volumetric flow of the catchers with configuration D outlets at different free stream velocities.

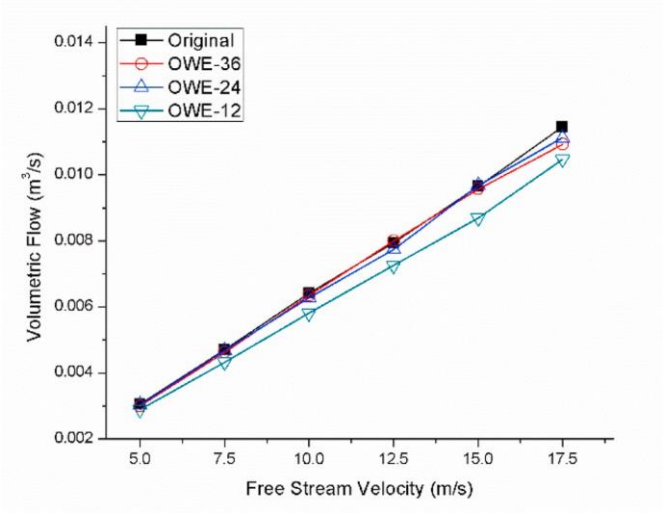

Fig. 16. Volumetric flow of the catchers with configuration E outlets at different free stream velocities.

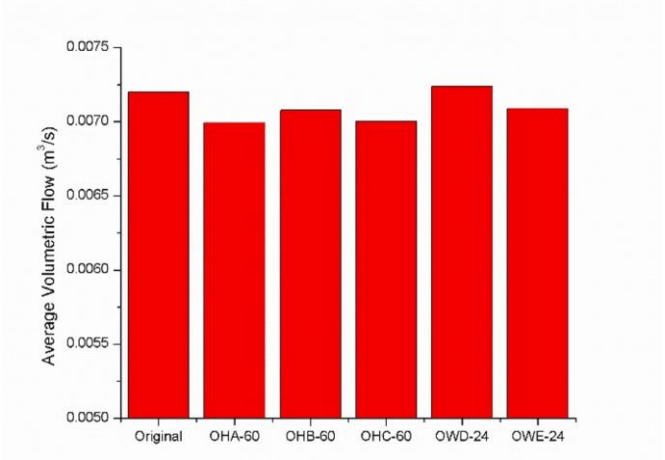

Fig. 17. Average volumetric flow for models that reduce the outlet opening by 50%.

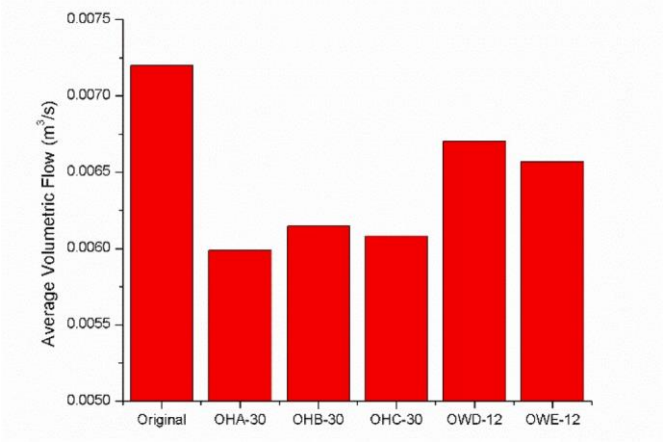

Fig. 18. Average volumetric flow for models that reduce the outlet opening by 75%.

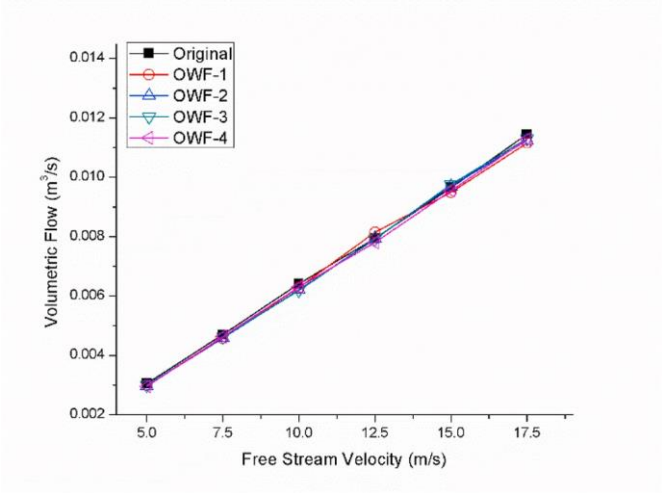

Fig. 19. Volumetric flow of the catchers with configuration F at different free stream velocities.

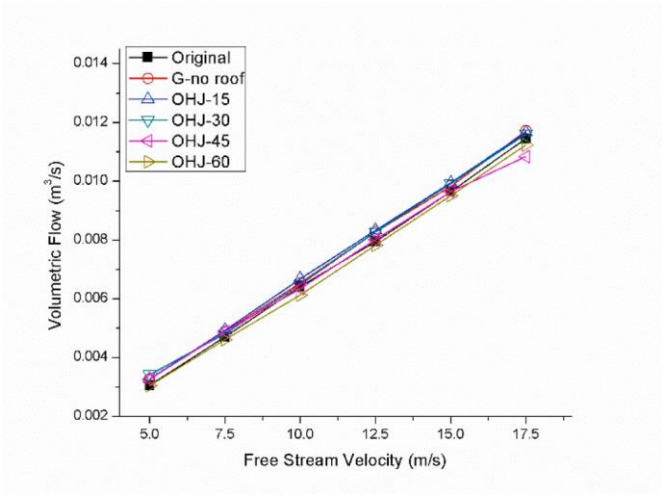

Fig. 20. Volumetric flow of the catcher with configurations G and J at different free stream velocities. increments of 15 mm.

Fig. 8 shows all the models of configuration J.

3. Meshing

The windcatcher is connected to an underground building. In the CFD modelling, the tower is placed in a domain split in two by a symmetry plane parallel to the wind direction, as can be seen in Fig. 9. Using a symmetry plane as a boundary condition significantly reduced the number of mesh elements needed and consequently the processing time needed for simulation. The domain has a height equivalent to 5H (where H is the height of the tower inside the simulated wind tunnel), a width equivalent to 2.5H from the symmetry plane and a length of 3H before the tower and 6H after. In general in the literature, when simulating typical buildings the size of the domains is usually larger. However, for wind towers, the nature of the flow is unique, because the flow that interacts with the tower and enters the building, also exits from the same right into the wake, which allows the use of smaller domains. Reducing the size of the domain is conventional when simulating this type of flow, and is used and documented in various manuscripts [28–33].

Being a very complex flow, many meshing settings were tested for different geometric configurations. After many considerations, a mesh formed only of tetrahedrons was selected. To ensure proper element size control for the mesh in the catcher's wake, a special control volume was set. This was used to assign very specific element sizes in one of the zones where there were more convergence problems caused by multiple vortex shedding. The control volume is 160 mm in length, by 180 mm in height, by 60 mm width from the symmetry plane to the deepest edge, and is placed 26 mm behind the tower.

Several convergence tests were done to determine a configuration where the results were consistent. This configuration was chosen carefully to try and avoid an excess of elements that could saturate the computer's bus, but also produce results that were not dependent on the mesh, especially in the zones with vortexes, like the wake and some areas inside the underground building. Initially, the same mesh configuration was used that had been employed in a parallel study and validated in wind tunnel testing. This helped to determine the values of the flow speed in the first cells adjacent to the walls. With this information, the whole mesh was configured to have mesh values of $Y+ = 1$, which resulted in a very dense mesh. In a second step, six more meshes were created with each one less dense than the previous with from 20% to 10% fewer elements. To reduce progressively the number of elements, the size of the elements in contact with the walls and the growth ratio of the areas close to the same increased with every mesh. To compare the performance of the different meshes, various variables in the simulations were compared. The first variable was the airflow captured by the wind tower, which was measured by two surface monitors in the vertical ducts: one in the ingress duct and another in the egress duct. In addition, various velocity profiles inside the underground building and outside the catcher were used to compare the flowfield as the mesh changed. From the seven meshes, the first being the finest and the seventh the coarsest, the fifth was the one selected for all the subsequent simulations.

Table 1 shows the element sizes for the different flow regions, and Fig. 10 shows the final mesh used in the CFD phase, with the named sections of the regions. The number of mesh elements changes as the shape of the outlets changed, but on average there were 4.75 million elements, having a maximum size of 0.03 m, and a 1.2 element growth rate over the great majority of the domain.

4. CFD

For the numerical simulation phase of the work, ANSYS Fluent was chosen as the tool to simulate the flow fields and this has been used by many researchers [14,19,20,34–36]. Finding a consensus about the right turbulence model to use to simulate the flow field inside and around the windcatcher proved not possible. This was mainly because of the large number of configurations found and documented in the literature [22, 34]. In preliminary tests, the same models used in different publications were tested. Various configurations of the k-ε turbulence model were used as in the work of Hosseinnia [19], Calautit [37], Heidari [35], and different configurations of the k-ω model were tested following the work of Dehghani [14], Hosseini [20], and Per´en [36]. To widen the search the k-kl-ω model was also used, even when this model is not often used in this type of flow. The comparison of results between the different turbulence models and the wind tunnel testing is not presented in this manuscript but will be published separately showing in more detail the strong and weak points of each turbulence model when simulating this type of flow.

Overall the SST k-ω and the k-kl-ω models achieved results closest to those obtained in the wind tunnel. In this case, the results were quite similar between both models. However, as the k-kl-ω needed more computer time, and there were no published papers that could support its selection, it was discarded. Thus the SST k-ω model was chosen to work with during all of the numerical simulation phase of the work. In all cases, the governing equations for mass conservation, momentum conservation, energy conservation, turbulent kinetic energy, energy dissipation rate, specific rate of dissipation, among many other variables

Table 2
Volumetric flow measured in all the models at the six different free stream velocities.

	1st free stream velocity (m^3/s)	2nd free stream velocity (m^3/s)	3rd free stream velocity (m^3/s)	4th free stream velocity (m^3/s)	5th free stream velocity (m^3/s)	6th free stream velocity (m^3/s)
Original	0.00305	0.0047	0.00642	0.00794	0.00966	0.01145
OHA-105	0.00306	0.00462	0.0062	0.00787	0.0095	0.01125
OHA-90	0.00313	0.00478	0.00627	0.0081	0.00937	0.0112
OHA-75	0.0031	0.00465	0.0064	0.00794	0.00932	0.01121
OHA-60	0.00309	0.00463	0.00636	0.00775	0.00919	0.01091
OHA-45	0.00296	0.00447	0.00584	0.00754	0.00885	0.01046
OHA-30	0.00266	0.004	0.0053	0.00662	0.00796	0.00939
OHB-105	0.00306	0.00474	0.00646	0.00812	0.00974	0.01123
OHB-90	0.00304	0.00466	0.00635	0.00808	0.00986	0.01176
OHB-75	0.00305	0.00465	0.00631	0.00807	0.00967	0.01148
OHB-60	0.00298	0.00456	0.00617	0.00798	0.0095	0.01125
OHB-45	0.00297	0.00446	0.00607	0.00763	0.00903	0.01056
OHB-30	0.00267	0.004	0.00538	0.00684	0.00835	0.00963
OHC-105	0.003	0.00461	0.00634	0.00801	0.0097	0.01167
OHC-90	0.00299	0.00461	0.0062	0.00809	0.00962	0.01151
OHC-75	0.00307	0.00456	0.00623	0.00773	0.00949	0.01114
OHC-60	0.00298	0.00462	0.00618	0.0078	0.00932	0.01114
OHC-45	0.00297	0.00449	0.00593	0.00754	0.00914	0.01056
OHC-30	0.00262	0.00396	0.00544	0.0068	0.00814	0.00956
OWD-36	0.0031	0.00474	0.00636	0.00824	0.00956	0.01164
OWD-24	0.003	0.00478	0.00639	0.00793	0.00977	0.01153
OWD-12	0.00292	0.00445	0.00605	0.00735	0.009	0.01047
OWE-36	0.003	0.00462	0.00634	0.008	0.00957	0.01092
OWE-24	0.00303	0.00467	0.00628	0.00774	0.00968	0.01112
OWE-12	0.00289	0.00432	0.00581	0.00726	0.00869	0.01047
G-no roof	0.00327	0.00488	0.00653	0.00827	0.00983	0.01171
OHJ-15	0.00327	0.00493	0.00667	0.00833	0.00995	0.01166
OHJ-30	0.00341	0.00481	0.00649	0.00827	0.00993	0.01161
OHJ-45	0.00325	0.00488	0.00634	0.00801	0.00965	0.01084
OHJ-60	0.00304	0.00461	0.00613	0.00782	0.00951	0.01123
OWF-1	0.00299	0.00458	0.00629	0.00814	0.0095	0.01115
OWF-2	0.00298	0.0046	0.00621	0.00793	0.0097	0.01124
OWF-3	0.003	0.00462	0.0062	0.00792	0.00976	0.0113
OWF-4	0.00296	0.00464	0.00631	0.00781	0.00956	0.01129

associated with the different turbulence models, were not modified and were used as found in the ANSYS Fluent User's Guide [38]. For the SST k-ω model the governing equations are as follow:

Mass conservation:

$\nabla \times (\rho \vec{v}) = 0$ (1) where ρ is density and $\vec{v}$ refers to the velocity vector.

Momentum conservation:

$$\nabla \times (\rho \vec{v} \vec{v}) = -\nabla p + \nabla \times (\bar{\tau}) + \rho \vec{g} + \vec{F} \quad (2)$$

In this equation, p represents the pressure, $\rho \vec{g}$ the gravitational force, $\vec{F}$ the external body forces, and $\bar{\tau}$ stands for the stress tensor:

$$\bar{\tau} = \mu \left[(\nabla \vec{v} + \nabla \vec{v}^{T}) - \frac{2}{3} \nabla \times \vec{v} I \right] \quad (3)$$

where μ stands for the molecular dynamic viscosity, and I the unit tensor. While the transport equations are:

$$\frac{\partial}{\partial x_i}(\rho k u_i) = \frac{\partial}{\partial x_j}\left(\Gamma_k \frac{\partial k}{\partial x_j}\right) + \tilde{G}_k - Y_k + S_k \quad (4)$$

$$\frac{\partial}{\partial x_i}(\rho \omega u_i) = \frac{\partial}{\partial x_j}\left(\Gamma_\omega \frac{\partial \omega}{\partial x_j}\right) + \tilde{G}_\omega - Y_\omega + D_\omega + S_\omega \quad (5)$$

In both equations, $\tilde{G}_k$ is the turbulent kinetic energy due to average velocity gradient, $\tilde{G}_\omega$ the generation of ω (dissipation). Γ_k represents the effective diffusivity of k, while Γ_ω the effective diffusivity of ω. Y_k and Y_ω stand for the dissipation of k and ω due to turbulence, while D_ω is the cross-dissipation. Finally S_k and S_ω are source terms defined by the users.

For all the catchers with different outlet configurations, there were six simulations carried out at six different free stream inlet velocities from 5 m/s to 17.5 m/s in increments of 2.5 m/s. For the domain outlet, a pressure outlet was set at 0 Pa. In addition, a second-order upwind scheme was adopted, and for pressure-velocity coupling, a Semi-Implicit Method for Pressure-Linked Equation was used. For the convergence of each simulation, all the standard values found in the ANSYS Fluent User's Guide [38] were used and so the values for the convergence criterion were 10^{-3} for all equations. In all cases, the iteration process was completed when the set convergence criteria were met and when the slope of the residuals' graphs was stable. Additionally, if the difference computed between the monitors that measured the flow in the vertical ingress duct and the vertical egress duct wasn't close to zero, the simulations weren't considered valid. In general, these conditions were met at between 400 and 550 iterations, depending on the flow speed; those with lower wind speeds converging after more iterations. Using five cores working in parallel, each simulation took from 3.5 h to 8.5 h to complete depending on the size of the mesh and the flow complexity on the wake. All the simulations were carried out in the same computer. This PC has an Intel Core i7 processor with 12 cores running at 4.2 GHz helped by a liquid cooling system and 64 GB of ram.

5. Results and discussion

Using the *SST k-ω* model, 33 outlet designs together with the original catcher were simulated at six different free stream velocities giving a

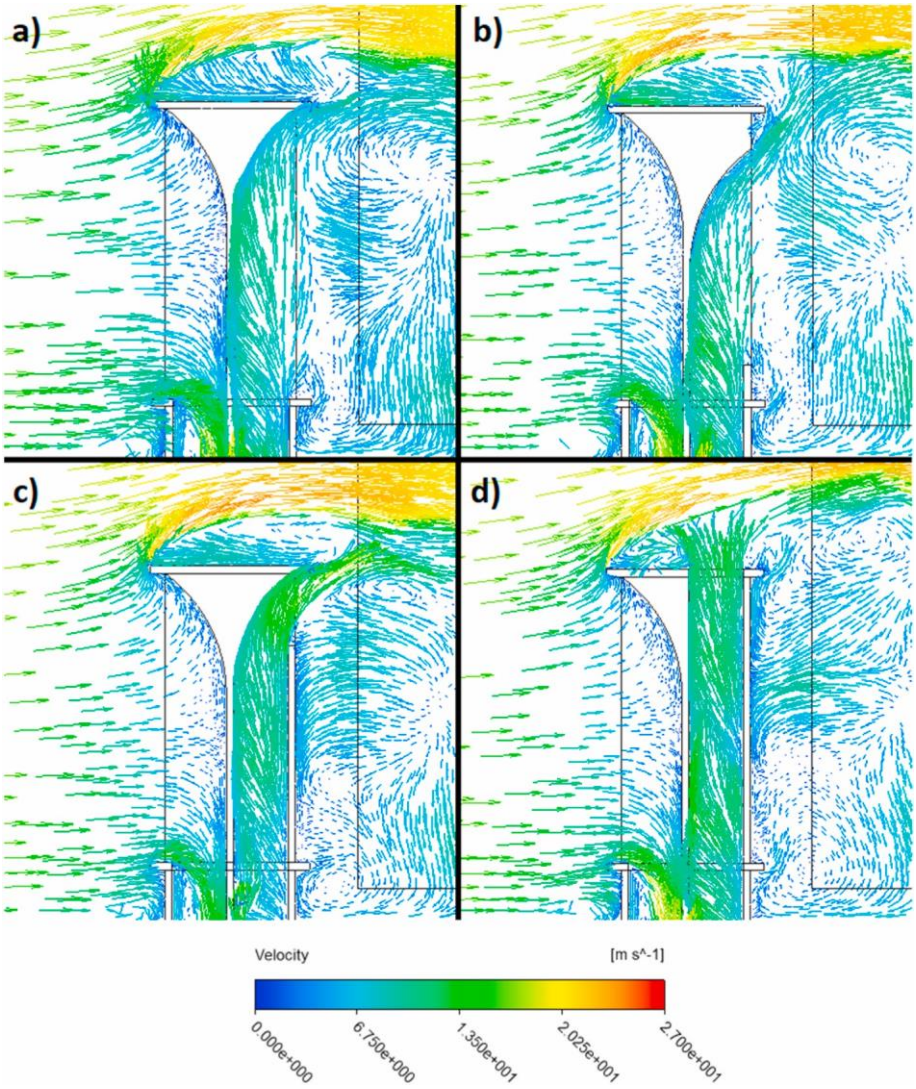

Fig. 21. Vector maps of the symmetry plane at 17.5 m/s of free stream velocity of models (a) Original, (b) OHB-90, (c) OHA-30, (d) OHG-15.

total of 204 converged simulations.

The volumetric flow computed for design configurations A, B, C at the six free stream velocities is shown in Figs. 11–13. As mentioned before they decrease the outlet size by shortening the height in decrements of 15 mm, but the openings are placed in different sections of the same space of the original opening. For these three configurations, 14 of the 18 models reduced the airflow through the ducts. Logic dictates that reducing the exit area would reduce airflow. However, the wind structures present in windcatchers, especially in the wake are very complex, and by changing the outlet placement it is possible to modify the behavior of the flow in that area to boost or reduce air evacuation from the ducts. Proof of this is seen in models OHB-105, OHB-90, OHB-75 and OHC-105, which were able to increase the volumetric flow on average by 0.23% up to 1.22%. This is a very modest increase and arguably statistically irrelevant, but it shows that reducing the exit area does not necessarily translate to a significant airflow decrement.

The airflow reductions are more significant in models OHA-30, OHB- 30 and OHC-30, which decreased the airflow on average by 16.85%, 14.70%, and 15.51% respectively, even when the outlet areas are larger than the cross-section area of the vertical duct that evacuates the air from the room. This duct has an area of 1080 mm^2 while the model outlets are of 1440 mm^2. The air comes from the ducts in a vertical direction and abruptly changes to a horizontal direction to meet the free stream of the main flow. It seems that the change of direction in the flow creates a large aerodynamic load that is hard for the windcatchers to overcome. However, the traditional designs mitigate this problem using a large size exit that creates a zone to help the air slowly change direction. Although having such a large exit area seems like an advantage, there is a limit where increasing the size of the opening does not necessarily translate to an airflow increment. Fig. 14 supports this assertion by showing the average flow for all the configurations at different length outlet openings. It is possible to see that for the first three opening height configurations there are very

small differences in the volumetric flow computed. Actually, on average over all the simulations, the openings of 105 mm only performed 0.37% worse than the original openings (120 mm), and the outlets of 90 mm only conducted 0.039% less air than the originals, which could indicate that for this particular case, it is not necessary to have an outlet that opens vertically more than 90 mm. In other words, having an outlet four times larger in area than the vertical ducts seems to offer good results, that don't improve much even if the opening is 5.33 times larger than the ducts. For the smaller outlets the percentage of airflow drops; the outlets with 75 mm, 60 mm, 45 mm, and 30 mm, reduce the average flow by 1.19%, 2.49%, 6.31%, and 15.68% respectively. These outlets are 3.33, 2.66, 2.0, and 1.33 times larger in area, respectively, than the cross-section of the vertical duct that evacuates the air from the building.

On average configurations A, B, C decreased the airflow at different rates. Configuration A decreased airflow on average over all the wind

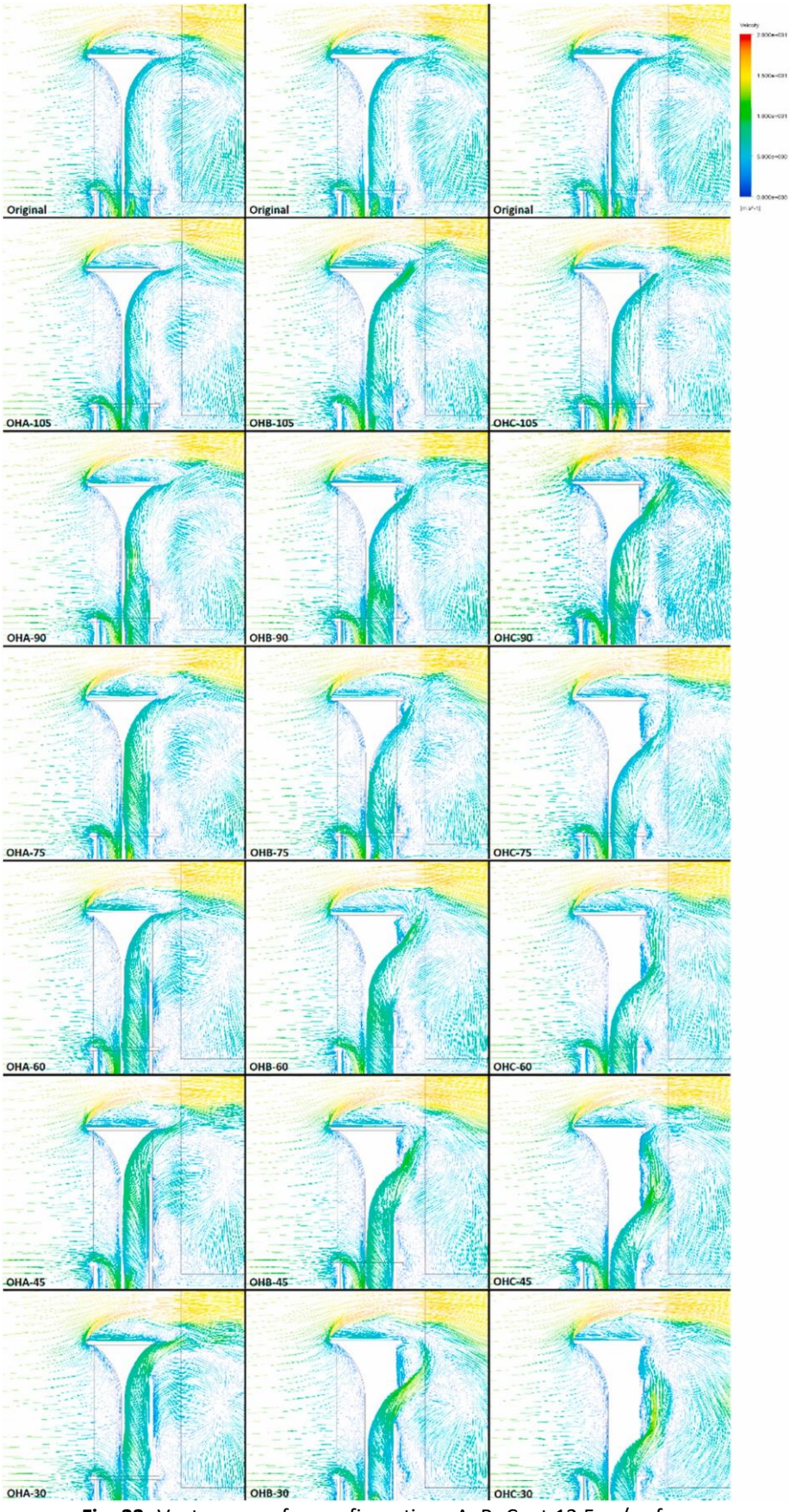

Fig. 22. Vector maps for configurations A, B, C, at 12.5 m/s of free stream velocity.

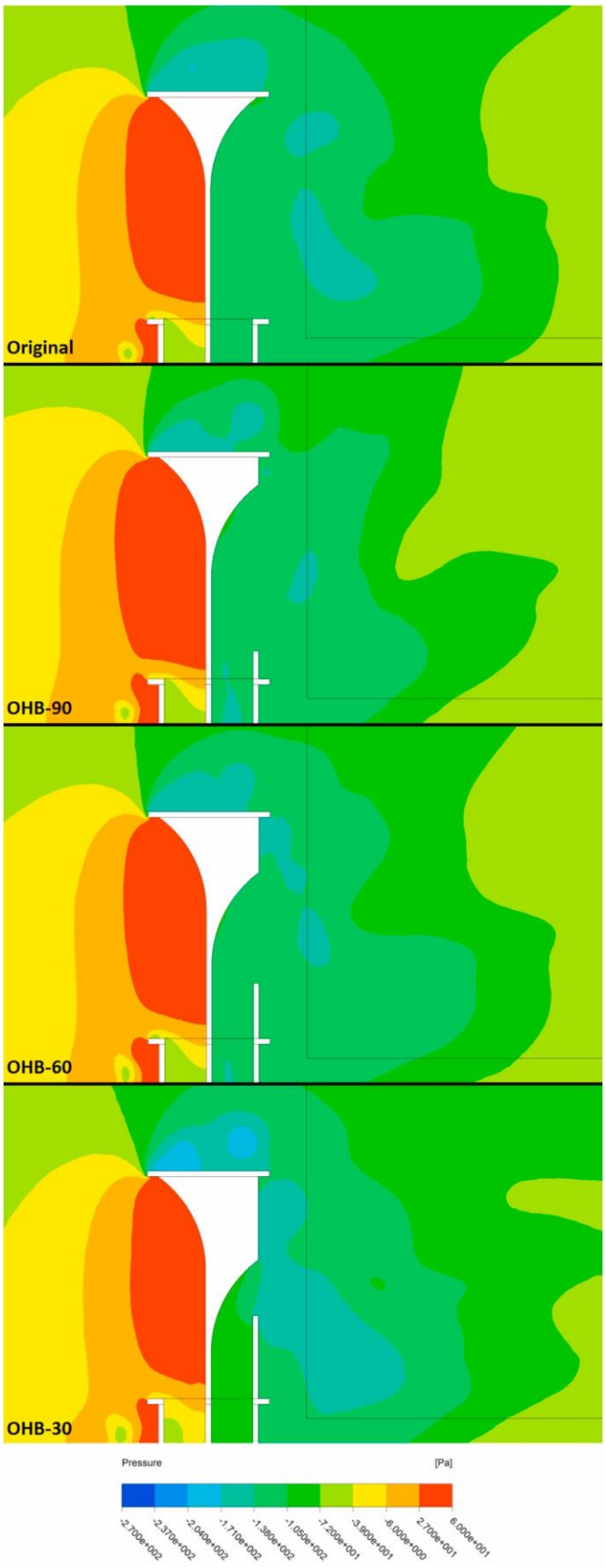

speeds and heights by 5.13%, configuration B reduced the flow on average by 3.45%, while configuration C by 4.46%, making the models closest to the top of the tower the ones that performed the worst, while those in the middle restrain the flow the least.

The volumetric flow for configurations D and E at the six free stream velocities is shown in Figs. 15 and 16 respectively. These configurations decrease the outlet width in decrements of 12 mm, but D starts to close from the sides, while E does it from the center.

Data from configuration D shows an average flow increment of 0.98% for model OWD-36, 0.44% for model OWD-24, but a 6.92% decrement in airflow for OWD-12. For configuration E every model decreases the airflow. OWE-36 restricts flow by 1.77%, OWE-24 by 1.64% and OWE-12 by 8.73%. Once again the six cases have a larger opening area than the cross-section of the vertical ducts. The openings with a total width of 36 mm have 4 times the area, those with 24 mm of total width are 2.66 times larger, and the ones with a total width of 12 mm are 1.33 larger in area than the vertical ducts.

To compare configurations A, B, C with configurations D and E, Fig. 17 shows a comparison of all the models that reduce the outlet opening area by 50%. This graph confirms previous observations and shows that for the first three configurations there is a decrement in flow. Model OHB-60 restrains the flow the least by 1.79%, while models OHA- 60 and OHC-60 reduce airflow by 2.93% and 2.75%. On the other hand, model OWD-24 improves the flow a modest 0.45%, showing that it is not necessary to have such a large outlet to achieve the best results. All that is needed is to place the outlet in the right spot, while model OWE-24 does the opposite and restrains airflow by 1.64%.

Fig. 18 compares the models that reduced the outlet area by 75%, to only one-quarter of the original opening. It repeats the behavior of the last graph but with more drastic drops in airflow, showing flow decrements from 6.92% to 16.85% in the worst case. All of this proves that it is necessary to do more research on ways to reduce losses in the performance of the windcatcher outlets to understand more deeply the interaction between the outlet and the flow and thus find the best possible configurations for the opening. The flow is so complex that even when reducing the outlet to one half, it is still possible to maintain the same airflow. To contribute to the understanding it was decided to test the configurations used in the vernacular architecture too, as a simple way to see if the columns present in the outlet have an effect on the volumetric flow.

Fig. 19 shows the volumetric airflow in the ducts when the outlet is obstructed by various numbers of columns. In every case, the flow was restricted by these configurations. Having 1, 2, 3 or 4 columns reduced the flow for every model on average by 1.56%, 1.27%, 1.21%, and 1.49% respectively. The columns reduced the opening area by 33.33%, 40%, 42.83% and 44.44% respectively, but there is no relation between the sizes of the openings and the reduction in airflow; the largest opening in fact had the more significant losses.

Fig. 20 shows the volumetric flow computed for configuration G, which has a vertical exit with no "roof" for the outlet duct, and configuration J that also has no roof but has the original opening shortened. For model G, it seems that avoiding the change of direction in the ducts from vertical to horizontal, and the presence of the low- pressure zone at the top of the catcher helped boost the airflow, which increased on average by 2.97%. For models OHJ-15 and OHJ-30 there is an even better scenario. On average they improve airflow by 3.65% and 3.02% respectively. Opening the exit more aided the air evacuating the tower to meet the main wind current outside the catcher, and boosted the flow. However, when the horizontal portion of the opening was larger, as in models OHJ-45 and OHJ-60, the effect was the opposite, decreasing the airflow by 0.53% and 2.04% respectively; the exiting current modified the wake structures and lost the effect of the suction at

Fig. 23. Scalar pressure maps of some representative cases of configuration B at the top of the tower. Table 2 shows the values of the volumetric flows computed in all the simulations.

12.5 m/s of free stream velocity.

Fig. 21 shows vector maps of the same free stream velocity at the symmetry plane of some of the most significant cases. Fig. 21a shows the

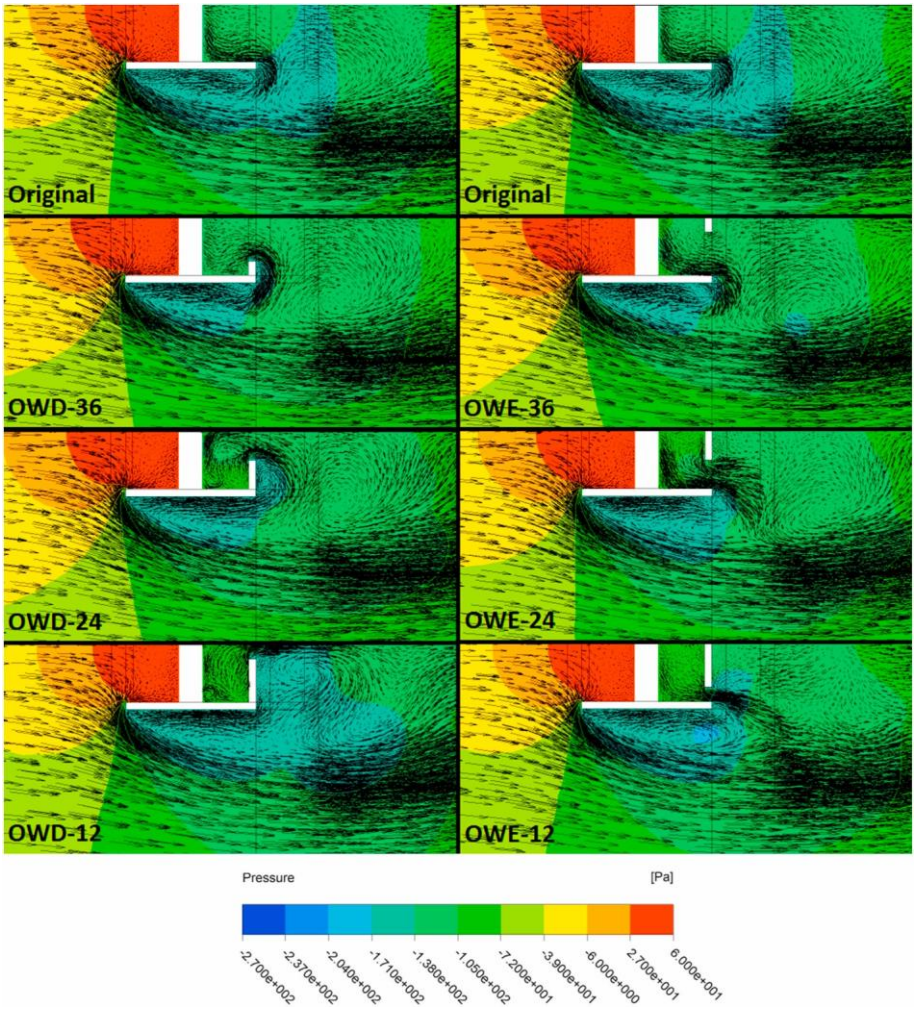

Fig. 24. Vector maps of configurations D and E at 12.5 m/s of free stream velocity with a background of the pressure field.

original design. As can be seen in the Figure, a large vortex is present next to the outlet. Some of the vectors from this vortex point into the outlet opening, and impede a free evacuation of air from the catcher. Inside the opening the vectors go straight up and curve out in the top, creating an egress stream at the very top of the tower. However, there is the presence of some small vectors that leave the catcher along the way. Fig. 21b shows one of the best performing horizontal outlet configurations (OHB-90). The vortex of the original case is also present in this configuration. Nevertheless, it seems to be pushed downstream just enough to let more vectors of smaller dimensions leave the tower before the air reaches the main

egress stream on top of the outlet. Fig. 21c shows one of the worst-performing models (OHA-30). In this case, the vortexes shown in Fig. 21a and b are also present, but they interact differently with the catcher. Clearly, the same egress stream at the top is present, but in this case, it is the only way for the air to leave the tower. This could explain the 16.85% reduction in the mass flow. By closing the area where the air evacuated the catcher and changed direction progressively, the mass flow reduced because the sudden change of direction on top of the tower needed more energy than the progressive change of direction in the previous cases.

Finally, Fig. 21d shows the vector map of the catcher with a vertical outlet. In this case, the vortex in the wake has limited interaction with the outlet. Instead, the egress flow interacts with the air on top of the tower and changes the way the boundary layer separates. By avoiding that last change of direction, the air leaves the catcher at a higher speed than in the previous cases. It also changes direction outside the tower, which could be the reason for the increment in the mass flow induced by the catcher. However, the present work does not seek to improve the performance of the windcatchers as the main target rather, the main interest is to learn which type of outlets reduce performance in order to avoid them in future projects.

The differences in the flow as the size and shape of the outlet changes, for configurations A, B and C, have been studied in more detail. Fig. 22 shows, at the symmetry plane, vector maps of the simulations with a free stream velocity of 12.5 m/s. The first column shows configuration A, where one can see that the flow has a tendency to egress from the catcher at the top of the outlet. The vectors have a tendency to stay inside the tower and even flow towards the interior wall, only to exit, in their great majority, at the top. This is mainly because of the presence of a large vortex in the wake that forces air inside the outlet. As the size of the opening increases, the position, size and shape of the vortex change very little. In contrast configuration B, shown in the second column, behaves differently even though the same vortex is present. As the size of the opening reduces and the top of the opening is dragged down, the vortex also moves down and reduces in size. At the same time, at the top of the catcher underneath the cantilever element, the formation of a new vortex can be seen, which unlike the original vortex, increases in size as the opening reduces. Configuration C shows similar behavior, although with notable differences because as the size of the opening reduces, a third large vortex becomes evident near the top of the towers. As the opening is dragged away from the top, this third vortex increases in size and the vortexes, described in configuration B, reduce their sizes.

Fig. 23 shows some representative cases of configuration B and how

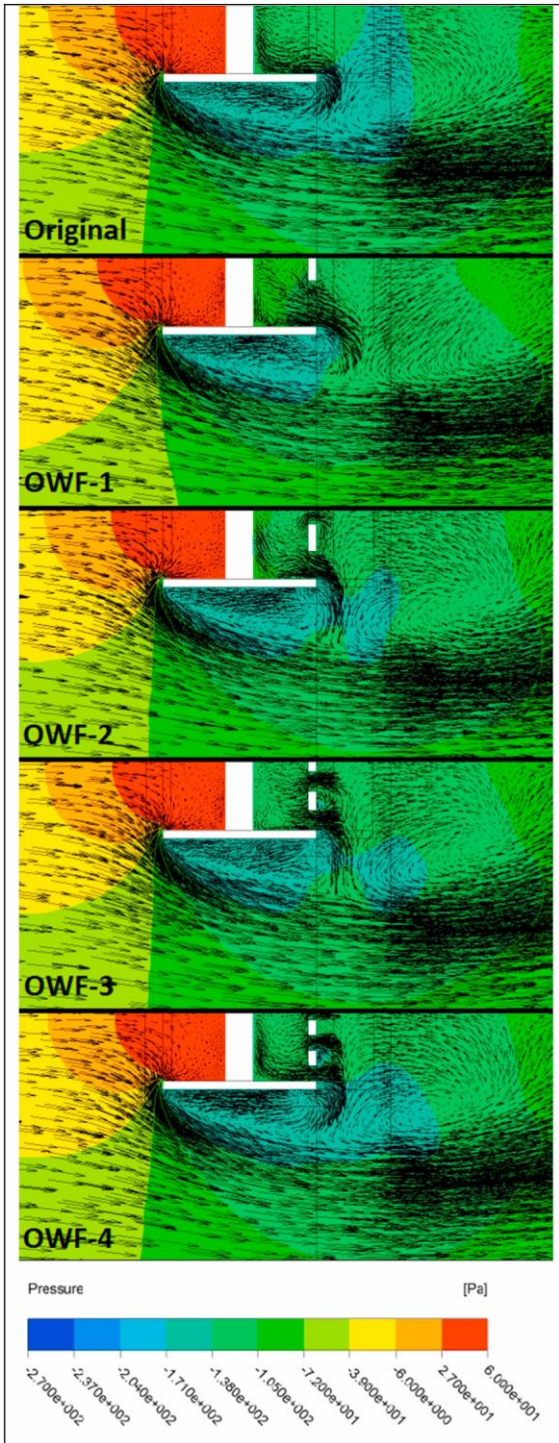

Figure 25 Vector maps with a pressure field background of configuration F at 12.5 m/s of free stream velocity.

the pressure field inside and around the tower changes as the vortex changes position. In the original design, two low-pressure zones are present, one on the top of the catcher and another in the wake. Changing the size and position of the outlet modifies considerably these two areas. The low-pressure zone on the top is pulled back as the outlet reduces its size. The one in the wake changes dramatically. First, when the outlet has a height of 90 mm, the zone reduces its size and moves down. Then, when the opening is 60 mm a new bubble forms in the location of the vortexes present on the vector maps. Finally, as the opening is at 30 mm, a large low-pressure zone matches the position of the vortexes in the vector maps.

Fig. 24 shows vector maps parallel to the main flow for configurations D and E. The plane shown is placed 40 mm under the top of the outlet opening and the pressure field is shown in the background at the same height. Note that only one half of the tower is on display because of the use of a symmetry plane used as a boundary condition. Once again, reducing the size of the openings changes considerably the pressure field and the overall behavior of the air. In the original model, the presence of a large low-pressure zone in the wake and to the side of the towers is observed. Two large vortexes are also present in the same places. Something remarkable is that at this plane a large amount of the egress flow that leaves the tower doesn't flow straight back. Instead, it flows against the main flow and enters the vortex present next to the windcatcher. Once the air enters the vortex, it recirculates and then joins the main stream. As the width reduces to 36 mm in both configurations, D and E, the low-pressure zone in the wake reduces its size considerably. However, the great majority of the air in this plane keeps on following the same path as before, moving first upstream, then recirculating, and finally joining the main flow moving downstream. When the opening width is 24 mm, the egress stream changes. In this case, the flow splits and one part of it moves upstream to the vortex next to the catcher, while the other part flows into the large vortex in the wake. In the OWD-24 case, a new vortex is observed in the wake in contact with the wall that reduces the width of the opening. This vortex takes the majority of the egress air, recirculates it and then feeds it to the previously described vortexes. When the opening reaches 12 mm the behavior of the flow is considerably different between both configurations. Model OWD-12 shows that the vortex in contact with the new wall increased in size. Now it consumes the exit stream and takes it to the vortex upstream, the vortex downstream and also to the mainstream. In parallel, model OWE- 12 changes the flow even further. The air that is evacuating from the catcher creates a stream that flows directly into the main flow, moving downstream with very few vectors moving upstream.

Traditional windcatchers have columns obstructing the openings, mainly to support the weight of the roof. Fig. 25 shows the flow field when the number of columns is changed from one to four. The plane on display is 40 mm below the top of the opening. As was the case in the configurations shown in Fig. 24, a large portion of the air evacuating from the tower creates a stream that

flows upstream to meet the vortex next to the catcher. However, as the number of columns increases the proportion of air that flows to the upstream vortex decreases and the flow tends to move towards the vortex in the wake.

Exploring a different type of outlet, configuration J was proposed to study the effects of using a vertical outlet on the performance of the windcatchers. Fig. 26 shows the flow inside and around the windcatchers when the roof has been partly removed to allow the air to evacuate from the building vertically. In the original design, there is the presence of a low-pressure zone on top of the tower due to boundary layer separation. The vertical exit tries to take advantage of that, but as can be seen (Fig. 26 -original) the low-pressure zone on the top reduces in size significantly in the presence of the egress stream. In parallel, the closure of the original outlet allowed the formation of a large low-

Fig. 25. 12.5 m/s of free stream velocity. Vector maps with a pressure field background of configuration F at pressure zone in the wake. Both low-pressure zones help the air exit the tower and as can be seen (Fig. 26 G-no roof) one portion of the flow moves towards the upstream low-pressure zone and the other portion downstream to meet the other low-pressure zone. Opening the original

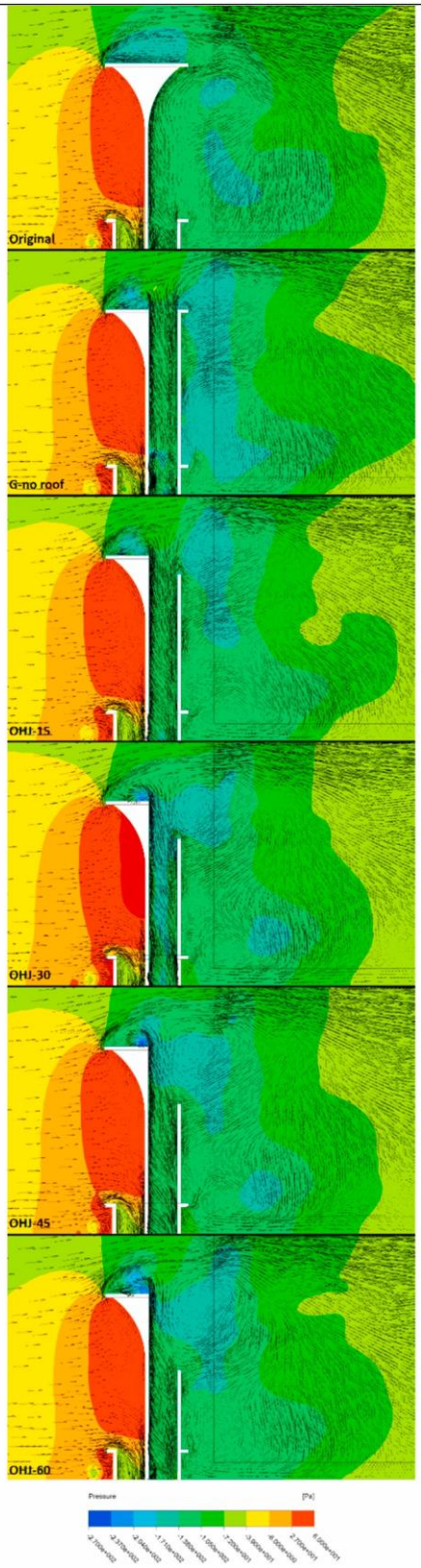

of

Figure 26 Vector maps with a pressure field background of configuration J at 12.5 m/s of free stream velocity.

Fig. 26. Vector maps with a pressure field background of configuration J at 12.5 m/s of free stream velocity.

outlet 15 mm transformed the wake, reducing the size of the low- pressure zones. Increasing the size of the opening to 30 mm reduced this even more and at the same time the vortex formed in the wake increased in size.

When the size of the side opening increased to 45 mm the size of this last-mentioned vortex increased and the presence of the same seems to be forcing air into the catcher. At the same time, the air tends to move towards the vortex on the top. Increasing the size of the horizontal opening to 60 mm increased both the size of the vortex and the low- pressure zone in the wake. However, the dynamic of the vortex forces air inside the tower. This reduces the portion of the duct that the air evacuating the tower uses to exit. At the same time, the air evacuating at the top moves upstream energizing the vortex on the top of the catcher. This combination of effects could be the reason why this configuration reduced the airflow inside the underground building.

All these different Figures illustrate the inefficiencies of the outlets of the traditional windcatchers and show which configurations are better to avoid when designing a windcatcher. At the same time, they prove that it is necessary to find a new way to evacuate the air from the wind tower in order to help the air evacuate straight into the wake to move downstream. In this way the possibilities of having air recirculating to the inlet openings reduce.

6. Conclusions

In this study, 204 cases of the scale model of a wind catcher with 33 different variations of its outlet openings were simulated connected to an underground building at six free stream velocities. In all cases, the size of the outlet opening was larger than the transversal area of the vertical ducts that evacuate air from the underground building. In the cases presented, it was observed that the height of the opening could be reduced until the opening area was four times the area of the vertical ducts without reducing flow considerably. When reducing the width of the outlet opening from the sides, the mass flow through the building didn't show major losses when the opening area was reduced from an equivalent of 5.33 times to 2.66 times the transversal area of the vertical ducts. The use of columns in the outlet was found in all cases to reduce the flow by a small margin. However, in the present work a relation was not found between the number of columns and the effects on the flow reductions. The use of vertical outlets showed some improvements in the majority of cases. By evacuating the air from the building vertically the mass flow increased up to 3.65% over the six free stream velocities.

In future work, the best performing configurations will be studied under different conditions and different variables of the flow will be reported.

CRediT authorship contribution statement

C.A. Varela-Boydo: Conceptualization, Methodology, Validation, Investigation, Resources, Data curation, Writing - original draft, Visualization, Supervision. **S.L. Moya:** Conceptualization, Methodology, Resources, Writing - review & editing. **R. Watkins:** Conceptualization, Writing - review & editing, Visualization.

Declaration of competing interest

The authors declare that they have no known competing financial interests or personal relationships that could have appeared to influence the work reported in this paper.

Acknowledgement

The first author gives thanks to the CONACYT for their financial support.

References

1. F. Jomehzadeh, et al., A review on windcatcher for passive cooling and natural ventilation in buildings, Part 1: indoor air quality and thermal comfort assessment, Renew. Sustain. Energy Rev. 70 (December 2016) 736–756, 2017.
2. M. Santamouris, Cooling the buildings – past, present and future, Energy Build. 128 (2016) 617–638.
3. M. Santamouris, D. Kolokotsa, Passive cooling dissipation techniques for buildings and other structures: the state of the art, Energy Build. 57 (2013) 74–94.
4. F. Manzano-Agugliaro, F.G. Montoya, A. Sabio-Ortega, A. García-Cruz, Review of bioclimatic architecture strategies for achieving thermal comfort, Renew. Sustain.
Energy Rev. 49 (2015) 736–755.
5. S. Suleiman, B. Himmo, Direct comfort ventilation. Wisdom of the past and technology of the future (wind-catcher), Sustain. Cities Soc. 5 (1) (2012) 8–15.
6. A. A'zami, Badgir in traditional Iranian architecture, Passiv. low energy Cool. built Environ. (May) (2005) 1021–1026.
7. M.N. Bahadori, M. Mazidi, A.R. Dehghani, Experimental investigation of new designs of wind towers, Renew. Energy 33 (10) (2008) 2273–2281.
8. V. Kalantar, Numerical simulation of cooling performance of wind tower (Baud- Geer) in hot and arid region, Renew. Energy 34 (1) (2009) 246–254.
9. Y. Bouchahm, F. Bourbia, A. Belhamri, Performance analysis and improvement of the use of wind tower in hot dry climate, Renew. Energy 36 (3) (2011) 898–906.
10. H. Montazeri, F. Montazeri, R. Azizian, S. Mostafavi, Two-sided wind catcher performance evaluation using experimental, numerical and analytical modeling, Renew. Energy 35 (7) (2010) 1424–1435.

11. A.A. Dehghan, M.K. Esfeh, M.D. Manshadi, Natural ventilation characteristics of one-sided wind catchers: experimental and analytical evaluation, Energy Build. 61 (2013) 366–377.
12. V.A. Reyes, F.Z. Sierra-Espinosa, S.L. Moya, F. Carrillo, Flow field obtained by PIV technique for a scaled building-wind tower model in a wind tunnel, Energy Build. 107 (2015) 424–433.
13. M. Afshin, A. Sohankar, M.D. Manshadi, M.K. Esfeh, An experimental study on the evaluation of natural ventilation performance of a two-sided wind-catcher for various wind angles, Renew. Energy 85 (2016) 1068–1078.
14. H. Dehghani Mohamadabadi, A.A. Dehghan, A.H. Ghanbaran, A. Movahedi, A. Dehghani Mohamadabadi, Numerical and experimental performance analysis of a four-sided wind tower adjoining parlor and courtyard at different wind incident angles, Energy Build. 172 (2018) 525–536.
15. O.S. Asfour, M.B. Gadi, Effect of integrating wind catchers with curved roofs on natural ventilation performance in buildings, Architect. Eng. Des. Manag. 2 (4) (Jan. 2006) 289–304.
16. H. Saffari, S.M. Hosseinnia, Two-phase euler-Lagrange CFD simulation of evaporative cooling in a wind tower, Energy Build. 41 (9) (2009) 991–1000.
17. V.A. Reyes, S.L. Moya, J.M. Morales, F.Z. Sierra-Espinosa, A study of air flow and heat transfer in building-wind tower passive cooling systems applied to arid and semi-arid regions of Mexico, Energy Build. 66 (2013) 211–221.
18. M.H. Ghadiri, N.L.N. Ibrahim, M.F. Mohamed, Performance evaluation of four- sided square wind catchers with different geometries by numerical method, Eng. J.
17 (4) (2013) 9–17.
19. S.M. Hosseinnia, H. Saffari, M.A. Abdous, Effects of different internal designs of traditional wind towers on their thermal behavior, Energy Build. 62 (2013) 51–58.
20. S.H. Hosseini, E. Shokry, A.J. Ahmadian Hosseini, G. Ahmadi, J.K. Calautit, Evaluation of airflow and thermal comfort in buildings ventilated with wind catchers: simulation of conditions in Yazd City, Iran, Energy Sustain. Dev. 35
(2016) 7–24.
21. N. Benkari, I. Fazil, A. Husain, Design and performance comparison of two patterns of wind-catcher for a semi-enclosed courtyard, Int. J. Mech. Eng. Robot. Res. 6 (5) (2017) 396–400.
22. H. Montazeri, F. Montazeri, CFD simulation of cross-ventilation in buildings using rooftop wind-catchers: impact of outlet openings, Renew. Energy 118 (2018)
502–520.
23. M. Sheikhshahrokhdehkordi, J. Khalesi, N. Goudarzi, High-performance building: sensitivity analysis for simulating different combinations of components of a two- sided windcatcher, J. Build. Eng. 28 (May 2019) 101079, 2020.
24. A. Zaki, P. Richards, R. Sharma, Analysis of airflow inside a two-sided wind catcher building, J. Wind Eng. Ind. Aerod. 190 (April) (2019) 71–82.
25. P. Nejat, F. Jomehzadeh, H.M. Hussen, J.K. Calautit, M.Z. Abd Majid, Application of wind as a renewable energy source for passive cooling through windcatchers integrated with wing walls, Energies 11 (10) (2018).
26. C.A. Varela-Boydo, S.L. Moya, Inlet extensions for wind towers to improve natural ventilation in buildings, Sustain. Cities Soc. 53 (Nov. 2019) 101933.
27. A.A. Badran, Performance of cool towers under various climates in Jordan, Energy Build. 35 (10) (2003) 1031–1035.
28. J.K. Calautit, B.R. Hughes, Wind tunnel and CFD study of the natural ventilation performance ofa commercial multi-directional wind tower, Build. Environ. 80
(2014) 71–83.
29. S.A. Ameer, H.N. Chaudhry, A. Agha, Influence of roof topology on the air distribution and ventilation effectiveness of wind towers, Energy Build. 130 (2016)
733–746.
30. B.R. Hughes, C.M. Mak, A study of wind and buoyancy driven flows through commercial wind towers, Energy Build. 43 (7) (2011) 1784–1791.
31. J.K. Calautit, D. O'Connor, B.R. Hughes, A natural ventilation wind tower with heat pipe heat recovery for cold climates, Renew. Energy 87 (2016) 1088–1104.
32. J.K. Calautit, B.R. Hughes, D. O'Connor, S.S. Shahzad, Numerical and experimental analysis of a multi-directional wind tower integrated with vertically-arranged heat transfer devices (VHTD), Appl. Energy 185 (2017) 1120–1135.
33. A.A. Elmualim, Effect of damper and heat source on wind catcher natural ventilation performance, Energy Build. 38 (8) (2006) 939–948.
34. T. van Hooff, B. Blocken, Y. Tominaga, On the accuracy of CFD simulations of cross-ventilation flows for a generic isolated building: comparison of RANS, LES and experiments, Build. Environ. 114 (2017) 148–165.
35. A. Heidari, S. Sahebzadeh, Z. Dalvand, Natural ventilation in vernacular architecture of Sistan, Iran; Classification and CFD study of compound rooms, Sustain. Times 9 (6) (2017).
36. J.I. Per´en, T. van Hooff, B.C.C. Leite, B. Blocken, CFD analysis of cross-ventilation of a generic isolated building with asymmetric opening positions: impact of roof angle and opening location, Build. Environ. 85 (2015) 263–276.
37. L.C. Haw, O. Saadatian, M.Y. Sulaiman, S. Mat, K. Sopian, Empirical study of a wind-induced natural ventilation tower under hot and humid climatic conditions, Energy Build. 52 (2012) 28–38.

38. Release, ANSYS Fluent User's Guide, 2017.